

# Acyclic Diene Metathesis Synthesis of Silylene- and Siloxane-Containing Conjugated Polymers and Macrocycles<sup>†</sup>

Narayan Mukherjee and Ralf M. Peetz\*

Center for Engineered Polymeric Materials (CePM), Department of Chemistry, City University of New York, Graduate Center and College of Staten Island, 2800 Victory Boulevard, Staten Island, New York 10314

Received March 26, 2008; Revised Manuscript Received June 11, 2008

**ABSTRACT:** Silylene- and siloxane-functional conjugated polymers and macrocycles could be synthesized via acyclic diene metathesis (ADMET) condensation of silylene- and siloxane-containing bis-styryl monomers. The organic conjugated segment formed was stilbene with all-trans-configured vinylene bonds. The flexible siloxane linkage resulted exclusively in dimeric macrocycles under the reaction conditions investigated, while the silylene linkage led to linear polycondensates with molecular weights  $M_n \sim 2000$ – $6000$  g/mol as determined by GPC and molecular weight distributions  $M_w/M_n \sim 1.4$ – $1.7$ . The microstructure was proven by means of  $^{13}\text{C}$  NMR,  $^1\text{H}$  NMR,  $^{29}\text{Si}$  NMR, and FTIR. Photophysical characterization of the products showed the participation of Si in the conjugation, in both the siloxanes and silylenes, with photoluminescence quantum efficiencies  $\sim 24$ – $28\%$  and blue light emission.

## Introduction

Conjugated polymers containing alternating conjugated segments and heteroatoms in the main chain are of considerable interest for a variety of applications. In particular, Si-containing conjugated systems have been investigated as potential materials for conductors, semiconductors, light emitters (especially blue light), and photovoltaic systems.<sup>1–5</sup> In these polymers made of alternating conjugated segments and silylene linkages, the conjugated segment, often an oligomeric mimic of a homologous conjugated polymer, features a discrete size and structure and hence defined electro-optical properties, in comparison to average distributions of fully conjugated segments in their polymeric analogues. The polymers feature  $\sigma$ – $\pi$ -conjugation, as the  $\text{sp}^3$ -hybridized silylene linkages allow for electronic delocalization through the  $\sigma$ -bonds, in addition to through-space interactions between the  $\pi$ -conjugated segments.<sup>1,6–9</sup>

Intramolecular charge transfer from photoexcited states reported for such systems may present an alternative to donor–acceptor architectures.<sup>10</sup> In addition to the electronic effects, the  $\text{sp}^3$ -link introduces significant flexibility into the polymeric chain, making it soluble and processable even at higher molecular weights. Properties, such as aggregation and solubility behavior, can be efficiently tuned by careful choice of substituent on the silylene spacer.

Olefin metathesis, especially acyclic diene metathesis (ADMET) polymerization, of silicon-containing polymers has been reported by Wagener and co-workers in particular.<sup>11</sup> However, hardly any attention has been focused on the synthesis of silicon-containing conjugated polymers via ADMET, as the vinyl derivatives of silicon compounds are usually not very reactive toward homometathesis due to steric and electronic effects, often with nonproductive cleavage of catalytic intermediates containing two silyl groups attached to adjacent carbon atoms. Select silicon-containing monomers undergo “silylative coupling”, as reported by Marciniak et al.<sup>12</sup> In 1997, Bazan and Miao reported on the ADMET of bis(vinylthienyl)silylenes using Schrock-type Mo-based alkylidene complexes. Polymers with intriguing optical properties were found; however, the monomers tended

to polymerize radically in a side reaction.<sup>13</sup> In this paper we present the ADMET of distyryl-functional silylenes (or silane) and siloxanes to produce linear polymers containing alternating *trans*-stilbene and silylene linkages and macrocyclic oligomers containing alternating *trans*-stilbene and disiloxane linkages. Earlier preliminary results yielded mixtures of siloxane- and silylene-containing materials and therefore remained inconclusive.<sup>14</sup> We are interested in synthesizing heteroatom-containing conjugated polymers with defined microstructures, using the functional-group-tolerant Grubbs-type Ru-based olefin metathesis initiators systems, and investigating the effect of molecular structure on the optoelectronic properties.

## Results and Discussion

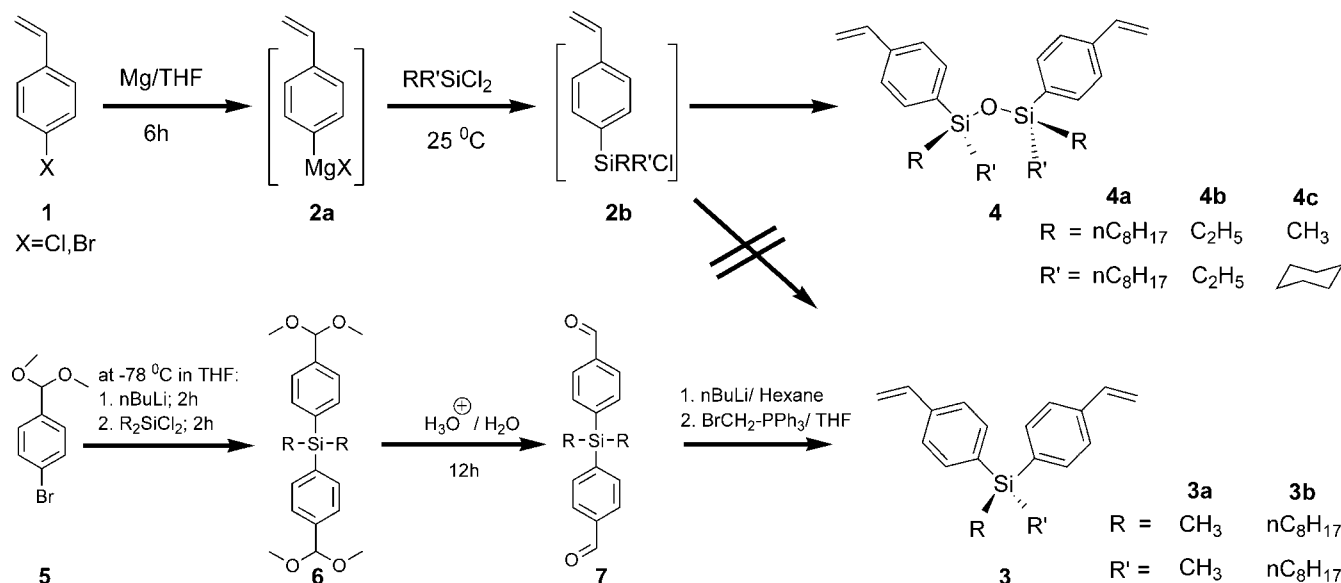
**Synthesis of Monomers.** In order to synthesize the silylene-containing bis-styryl monomers of the type **3a** and **3b**, a synthetic strategy, starting from *p*-bromostyrene (**1**), was followed as reported by Kim et al. (Scheme 1).<sup>3</sup> The Grignard reagent **2a** was prepared in situ from **1** or *p*-chlorostyrene by reaction with flame-dried magnesium metal in anhydrous THF at ambient temperatures. **2a** was then reacted with a respective dichlorodialkylsilylene ( $\text{RR}'\text{SiCl}_2$ ) to afford the monomer **3**, after work-up with 0.1 M HCl. However, we were not able to synthesize the targeted monomers **3** by this method. Rather, mainly monomers of type **4** were isolated, containing a siloxane unit between the terminal styryl units. A possible explanation is that after the first substitution step with  $\text{RR}'\text{SiCl}_2$  intermediate **2b** is formed. The remaining Si–Cl on **2b** is less reactive due to the aromatic substitution on Si. This Si–Cl hydrolyzes to Si–OH during the aqueous work-up and subsequently condenses with another Si–OH to form the siloxane unit. This is supported by detailed microstructure analysis (see below). The synthetic approach was attempted for different  $\text{RR}'\text{SiCl}_2$  with  $\text{R} = \text{R}' = n$ -octyl,  $\text{R} = \text{R}' = \text{ethyl}$ , and  $\text{R} = \text{methyl}$  with  $\text{R}' = \text{cyclohexyl}$ . With longer alkyl chain substitution (*n*-octyl), almost exclusively siloxane-containing monomer **4a** was isolated rather than **3b**, whereas using  $\text{R} = \text{R}' = \text{methyl}$  resulted in a mixture of both silylene **3a** and siloxane (type **4**, specific example not shown) that could not be effectively separated into its components.

Careful  $^{29}\text{Si}$  NMR spectra (see below) clearly identified the siloxane as opposed to silylene. Consequently, another synthetic approach to monomers of type **3** was followed: The diacetal of

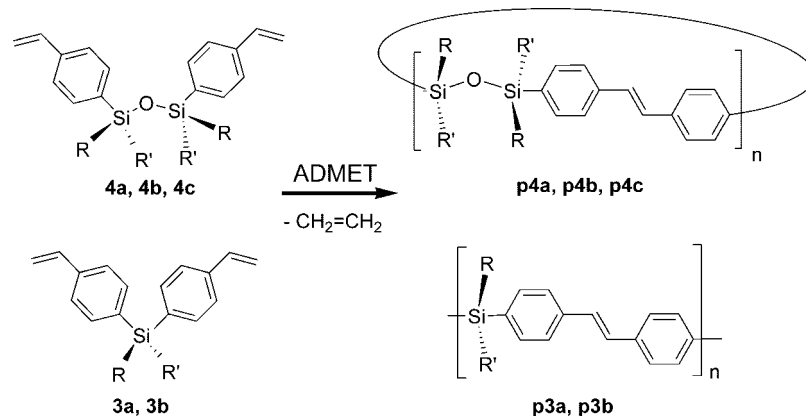
\* To whom correspondence should be addressed: phone 718-982-3928; fax 718-982-3910; e-mail peetz@mail.csi.cuny.edu.

<sup>†</sup> Dedicated to Joseph P. Kennedy on behalf of his 80th birthday.

Scheme 1. Syntheses of Monomers: Silylenes (3) and Siloxanes (4)



Scheme 2. ADMET of Silylenes (3) and Siloxanes (4)



*p*-bromobenzaldehyde (**5**) was lithiated with butyllithium at  $-78\text{ }^{\circ}\text{C}$ , followed by dropwise addition of  $\text{RR}'\text{SiCl}_2$ , yielding **6**.<sup>15</sup> A small excess of **5** was used to ensure the reaction of all  $\text{Si}-\text{Cl}$ . The acetals of compound **6** were removed by refluxing in acidic condition to afford dialdehyde **7**, which was then converted into monomer **3** via a standard Wittig reaction. This approach yielded exclusively silylene monomers **3a** and **3b** without traces of the respective siloxanes. This method not only led to 98% pure distyryldialkylsilylene but also resulted in higher overall monomer yields.

**Acyclic Diene Metathesis (ADMET) of Siloxane-Containing Monomers 4a, 4b, and 4c.** The ADMET polycondensation was successfully carried out both for monomers of the type **3** and **4** using ruthenium-based “Grubbs–Hoveyda second generation” [(1,3-bis(2,4,6-trimethylphenyl)-2-imidazolidinylidene)dichloro(*o*-isopropoxyphenylmethylene)ruthenium] ( $\text{C}_{31}\text{H}_{38}\text{Cl}_2\text{N}_2\text{ORu}$ ) and “Grubbs second generation” [1,3-bis(2,4,6-trimethylphenyl)-2-imidazolidinylidene)dichloro(phenylmethylene)(tricyclohexylphosphine)ruthenium] ( $\text{C}_{46}\text{H}_{65}\text{Cl}_2\text{N}_2\text{PRu}$ ) alkylidene complexes (Scheme 2). To explore the scope of this approach, temperature, time, and amount/type of alkylidene complexes were varied. Representative results of these polycondensations are summarized in Table 1.

In all cases, the reaction solutions remained homogeneous mixtures during the entire period of reaction; only a color change could be observed. Using octyl-substituted siloxane **4a**, almost

Table 1. ADMET of Siloxanes (4) in Toluene Using Grubbs–Hoveyda Second Generation Catalyst

entry	[catalyst] (mM)	[monomer] (mM)	time (h)/ temp ( $^{\circ}\text{C}$ )	yield (%)	$M_n$ (g/mol)/MWD
<b>p4a</b>					
1–3	5–16	130–320	18–60/30–40	n.a.	mainly monomer
4	6.2	245	18/48	89	1360/1.47
5	6.5 <sup>a</sup>	260	18/52	87	1400/1.25
6	1.6	164	18/50	87	1400/1.24
7	0.8	150	18/50	86	1410/1.25
8	0.3 <sup>b</sup>	170	18/50	n.a.	mainly monomer
<b>p4b</b>					
1	1.1	270	18/50	91	610/1.59
2	0.6	230	18/60	95	730/1.53
<b>p4c</b>					
1	2.3	230	18/50	91	940/1.02
2	4.8	194	18/50	95	940/1.02
3	4.3	170	12/50	92	800/1.02
4	5.0	200	18/60	88	980/1.02

<sup>a</sup> Catalyst: Grubbs second generation. <sup>b</sup> Catalyst: Grubbs first generation.

no product formation was observed at reaction temperatures  $30\text{--}40\text{ }^{\circ}\text{C}$  (#1). At  $\sim 48\text{--}50\text{ }^{\circ}\text{C}$ , however, the reactions resulted in product with isolated yields of  $\sim 86\text{--}89\%$  condensate, regardless of monomer/catalyst ratio (varied from  $\sim 200/1$  (#7) to  $\sim 10/1$  (#2)), using Grubbs second generation or Grubbs–Hoveyda second generation catalysts (#5 vs other entries, respectively). Only the Grubbs first generation complex

**Table 2. ADMET of Silylenes (3) in Toluene Using Grubbs–Hoveyda Second Generation Catalyst**

entry	[cat.] (mM)	[monomer] (mM)	time (h)/ temp (°C)	yield (%)	$M_n$ (g/mol)/MWD
<b>3b</b>					
1	4	200	18/55	95	6050/1.73
2	4	200	10/55	90	3700/1.43
3	1	280	18/60	n.a.	1530/1.00 <sup>b</sup>
4	3	200	18/65	89	5000/1.52
<b>3a</b>					
1	5	280	18/50	90	2250/1.44 <sup>a</sup>
2	5	250	18/50	85	2600/1.38 <sup>a</sup>

<sup>a</sup> THF-soluble product fraction. <sup>b</sup> Analysis of trace amount of one oligomer fraction; see Figure 1.

did not seem to be active enough under comparable conditions (#8). Reactions were usually continued for 18 h, and longer reaction times such as 60 h (# 3) at 30 °C did not result in higher condensate yields. A time-dependent <sup>1</sup>H NMR study of this particular reaction (**p4a**) revealed the presence of only trace amounts of vinyl functionality after only 60 min reaction time, indicating reaction completion.

ADMET of the siloxane monomers **4b** and **4c** yielded analogous results (Table 1), i.e., isolated condensate yields ~88–95% with ratios monomer/catalyst ~245/1–380/1 and ~40/1–100/1, respectively, all at temperatures at or above 50 °C. ADMET results of the homologue siloxane monomer with R = R' = methyl are not presented due to the low purity of the monomer (a mixture of silylene and siloxane, see above).

**ADMET of Silylene-Containing Monomers 3a and 3b.** ADMET polycondensation of silylene monomers **3a** and **3b** was carried out under the same conditions. In these cases, however, in addition to the color change a significant increase in viscosity of the reaction mixture could be observed after ~6–8 h, together with subsequent precipitate formation in several examples. Table 2 summarizes the results.

The ratio monomer/catalyst was varied between ~50/1 and 280/1. Only results from reactions at temperatures ~50–60 °C are reported for these systems. The yields of isolated product were not significantly different from yields in materials **p4**, varying from ~89 to 95%. The only significant differences observed lay in the molecular weights (see below).

**Molecular Weights of Monomers and Polymers.** Molecular weights of monomers and products were determined relative to polystyrene standards, and the traces for the differential refractive index (DRI) detector response are shown for all monomers and representative ADMET condensation products (Figure 1). The experimental molecular weights  $M_n$  and polydispersities  $M_w/M_n$  (PDI) of the ADMET products are listed in Tables 1 and 2. Table 3 compares theoretical and experimental values for the monomers.

A narrow monomodal trace was observed for each monomer (a trace of a higher molecular weight impurity was observed for **4b**). The experimental molecular weights for monomers of type **3** were slightly higher than the theoretical values, whereas the respective values for monomers **4** were significantly lower, most likely a consequence of the highly flexible Si–O–Si linkage.

In all cases, a productive ADMET reaction was indicated by a clear increase in molecular weight of product compared to monomer. However, in the case of products **p4a–c**, narrowly distributed, sometimes nearly monomodal traces were observed, indicating formation of one major product in every case. Shoulders from higher-molecular-weight components are rather insignificant. Considering the polycondensation nature of this reaction, it is highly unlikely that these product traces are representative of linear polymer chain mixtures. Because of the flexible Si–O–Si linkage, macrocyclic rings must have formed.

Ring–chain equilibria are common in ADMET polycondensations, in particular using flexible diene monomers.

In the case of products **p3a,b**, the molecular weight distributions are more typical of polycondensates. In the case of **p3b**, molecular weights were highly dependent on reaction conditions. With a high monomer/catalyst ratio of ~280/1, mainly unreacted monomer was recovered, together with one monomodal higher molecular weight fraction of  $M_n \sim 1530$  g/mol ( $M_w/M_n \sim 1.00$ ). This fraction is also observed in all the higher-molecular-weight polycondensation mixtures and most likely may be attributed to one specific oligomer formed. Other  $M_n$  dependencies follow the expected trends: lower ratios monomer/catalyst result in lower molecular weights (#1 vs #4, respectively), as do shorter reaction times (#1 vs #2, respectively). With increasing molecular weight, the relative amounts of monomer and shorter oligomers clearly decrease as expected. The maximum molecular weight isolated was ~6050 g/mol with PDI ~ 1.7 (#1). In the case of **p3a**, ADMET of **3a** led to a formation of a precipitate after ~1 h reaction time. The isolated product showed a low solubility in common solvents, such as toluene, THF, and CHCl<sub>3</sub>. As a result, the measured  $M_n$  of ~2250 (PDI ~ 1.4) is most likely over-representing the lower-molecular-weight fractions of the sample. The lower solubility is due to short methyl groups compared to the longer octyl chains in the case of **p3b**.

**Microstructure via NMR and IR.** All monomers and ADMET products were characterized by <sup>1</sup>H, <sup>13</sup>C, and <sup>29</sup>Si NMR. Representatively, the <sup>1</sup>H NMR spectra of **3b**, **4a**, **p3b**, and **p4a** with R, R' = *n*-octyl are depicted in Figure 2 and will be discussed.

The two vicinal protons =CH<sub>2</sub> from the vinyl end groups in **3b** and **4a** exhibit two characteristic doublet resonances at ~5.79 and 5.75 ppm for the exo protons ( $J \sim 17$  Hz) and ~5.26 and 5.25 ppm for the endo protons ( $J \sim 11$  Hz), respectively. The third proton –CH= of the end groups in **3b** and **4a** is observed as a quartet at ~6.72 and 6.70 ppm, respectively. The vinyl protons of **3b** show small but significant downfield-shifted resonances compared to **4a**. This, a consequence of silylene vs siloxane linkage, is observed as a trend in all monomers investigated. Resonances from the aromatic protons are observed at ~7.3–7.6 ppm. The protons from the octyl chains are observed as resonances at –0.5 to 1.6 ppm. The resonance integral ratios octyl protons/vicinal vinyl protons corresponded roughly to 34/4 for **3b** and 68/4 for **4a**, respectively, the presence of Si impacting the quantitative accuracy.

The <sup>1</sup>H NMR spectra of **p3b** and **p4a** show distinct changes relative to their respective monomers. The formation of product is marked by the appearance of a resonance at ~7.14 and 7.13 ppm, respectively, indicating the formation of the vinylene bond of the new *trans*-stilbene unit. The value for chemical shift of the internal vinylene protons in pure *trans*-stilbene is reported as ~7.14 ppm.<sup>16</sup> As this resonance appears, the resonances from the terminal vinyl groups (~5.3, 5.8, and 6.7 ppm; see above) in the monomers gradually decrease. No resonance was observed at ~6.5 ppm (reported value for the internal vinylene proton signals in *cis*-stilbene), indicating exclusively *trans* configured vinylene bonds. Resonances from the aliphatic protons were marked by a peak broadening relative to the respective monomers. Importantly, even in the case of **p3b** with  $M_n \sim 6050$  g/mol significant resonances from residual vinyl protons could be observed. In contrast, samples of **p4a** with  $M_n \sim 1400$  g/mol showed insignificant signal intensity from residual vinyl protons. This general observation is consistent for all systems **3** and **p3** vs **4** and **p4** and supports the formation of cyclic ADMET products in the case of the siloxane-based systems **p4**, as there is no terminal vinyl functionality in such case. The “backbiting” of two chain ends is possible for the siloxane-based systems due to the longer and highly flexible Si–O–Si



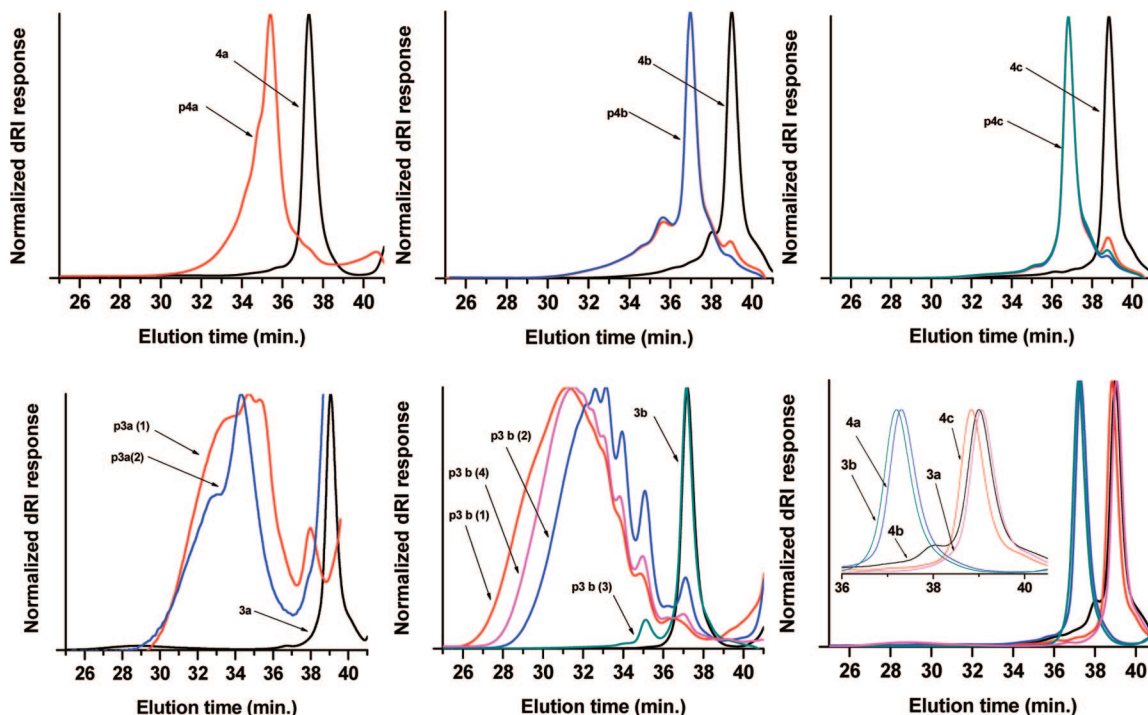


Figure 1. GPC traces of silylenes (**3**), siloxanes (**4**), and their respective ADMET condensates (**p3** and **p4**).

Table 3. Theoretical and Experimental Molar Masses of Silylenes (**3**) and Siloxanes (**4**)

monomer	$M_n$	
	theor	expt (MWD)
<b>3a</b>	264	288 (1.02)
<b>3b</b>	460	621 (1.04)
<b>4a</b>	731	629 (1.01)
<b>4b</b>	366	301 (1.04)
<b>4c</b>	474	313 (1.02)

linkage, which is absent in the case of silylene-based systems. The formation of discrete rings would also explain the unique GPC traces with only one main product, featuring unity as the PDI. In the systems **p3** chain end vinyl groups and vinyl groups from residual monomers could not be distinguished. But the presence of chain end functional vinyl groups is expected in linear polycondensation product mixtures. In fact, the integration the proton resonance intensity from terminal vinyl groups vs internal vinylene bonds yields additional insight into the molecular weight  $M_n$  of a sample. In the case of the depicted **p3b**,  $f(\delta(7.14 \text{ ppm}))/f(\delta(5.2\text{--}5.9 \text{ ppm})) = \sim 13$ , corresponding to a degree of polymerization  $\sim 26$  with  $M_n \sim 11\,232 \text{ g/mol}$  ( $M_n \sim 6050 \text{ g/mol}$  in GPC vs polystyrene standards, #1 Table 2). From the presented data we cannot, however, exclude the possibility of minor cyclic components in the ADMET products **p3**.

$^{29}\text{Si}$  NMR proved to be a very valuable tool to distinguish between silylene and siloxane species. Figure 3 depicts  $^{29}\text{Si}$  spectra for all monomers and ADMET products.

In all three siloxane monomers **4a–c** the  $^{29}\text{Si}$  resonance appeared at positive  $\sim 6.04\text{--}8.04 \text{ ppm}$ , whereas the silylenes **3a,b** were observed at negative ppm ( $\sim -8.75$  and  $-6.84 \text{ ppm}$ , respectively). Analogue values from the literature are in support: The  $^{29}\text{Si}$  resonance for  $(\text{CH}_3)_2\text{Si}(\text{C}_6\text{H}_5)_2$  and  $[(\text{C}_2\text{H}_5)_3\text{Si}]_2\text{O}$  were reported at  $\sim -9.4$  to  $-7.5 \text{ ppm}$  and  $+9.11 \text{ ppm}$ , respectively.<sup>17</sup> The respective ADMET products follow the same trend. The Si resonances for **p4a–c** were observed at  $\sim 6.21$  to  $8.84 \text{ ppm}$ , compared to  $\sim -9.68$  to  $-6.83 \text{ ppm}$  for the respective **p3a** and **p3b**. The existence of a single resonance in the product spectra, together with the other analytical data, indicates that the Si

centers have not been altered during the ADMET reaction with the Ru complex. The differences between monomers and ADMET products indicate a significant different electronic effect from the stilbene unit formed vs the styryl unit in the monomers.  $^{29}\text{Si}$  resonances from residual monomers residue could not be observed. The **p3a** spectrum was acquired in solid state due to significantly lower solubility and thus shows broader signals. Table 4 summarizes chemical shifts of the  $^{29}\text{Si}$  NMR resonances.

Further evidence of the different nature of monomer **3b** vs **4a** came from quantitative  $^{13}\text{C}$  NMR measurements. Table 5 summarizes the results.

In **4a** measured signal intensities from the side chains (1–8) are close to the calculated values or slightly higher, whereas the corresponding values for **3b** are slightly lower than the calculated values. In addition, the flexible Si–O–Si unit obviously leads to more rapid relaxations overall, resulting in higher signal ratios relative to the internal standard. For internal calibration, the measured intensities of the  $=\text{CH}_2$  carbon from the vinyl units were normalized to the theoretical value. Even the aromatic carbons seemed to be affected by this high degree of freedom, showing larger relative intensities for **4a** compared to **3b**.

FT-IR spectroscopy complemented the overall analytical picture—allowing the determination of distinct differences between the type **3** and type **4** monomers as well as between any monomer and its respective ADMET condensate. Figure 4 illustrates this for a select region of the FT-IR spectra of **4a**, **3b**, **p4a**, and **p3b**.

Si–CH<sub>2</sub> wagging was observed at  $\sim 1207 \text{ cm}^{-1}$ , Si–phenyl stretching at  $\sim 1105 \text{ cm}^{-1}$ , and broad Si–O–Si stretching at  $\sim 1025\text{--}1075 \text{ cm}^{-1}$  for **4a–c** and **p4a–c**. The terminal vinyl bonds show a C=C stretching with conjugation at  $\sim 1630 \text{ cm}^{-1}$  as well as the sharp out-of-plane (oop) deformations at  $\sim 987$  and  $\sim 906 \text{ cm}^{-1}$ . The ADMET reaction leads to overall broader, less intense aromatic C–H oop vibrations at  $\sim 820 \text{ cm}^{-1}$  compared to monomers at  $\sim 827 \text{ cm}^{-1}$ , whereas aliphatic C–H rocking at were more intense at  $\sim 700 \text{ cm}^{-1}$  vs  $\sim 697 \text{ cm}^{-1}$ , respectively. The most characteristic change occurred in the C=C stretching—after ADMET reaction, the degree of disap-

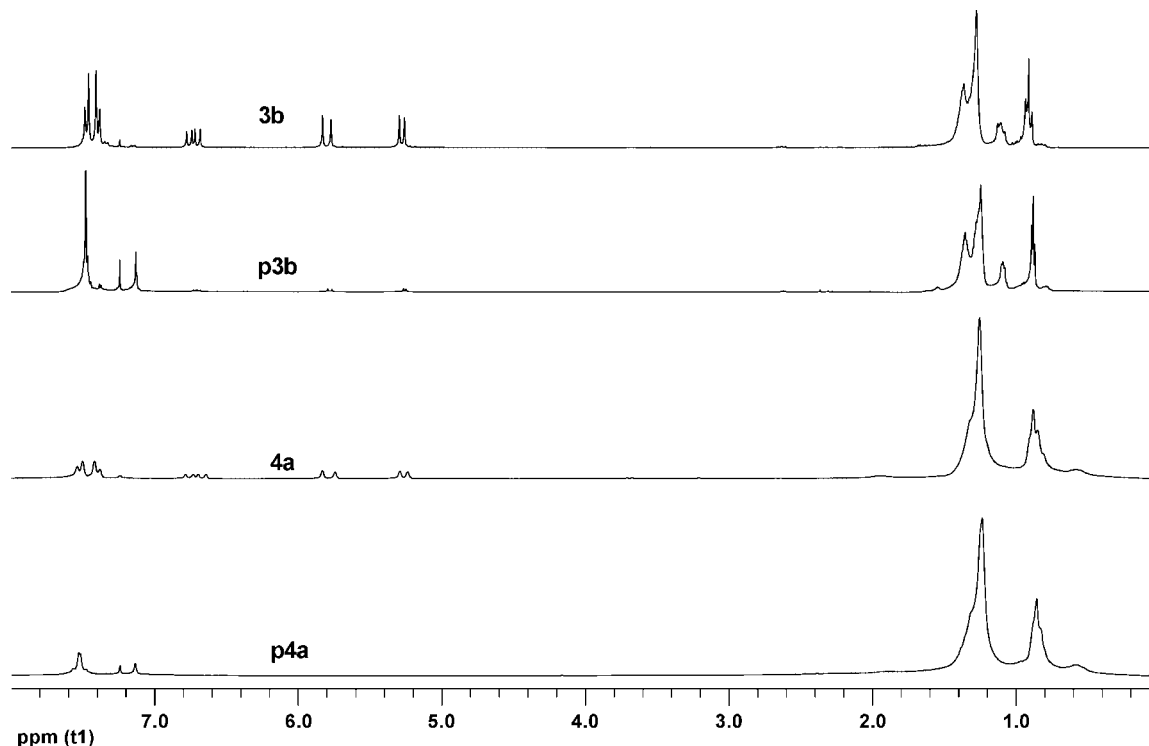


**Figure 2.**  $^1\text{H}$  NMR spectra (600 MHz in  $\text{CDCl}_3$ ) of silylenes (**3b**), siloxanes (**4a**), and their respective ADMET condensates (**p3b** and **p4a**).

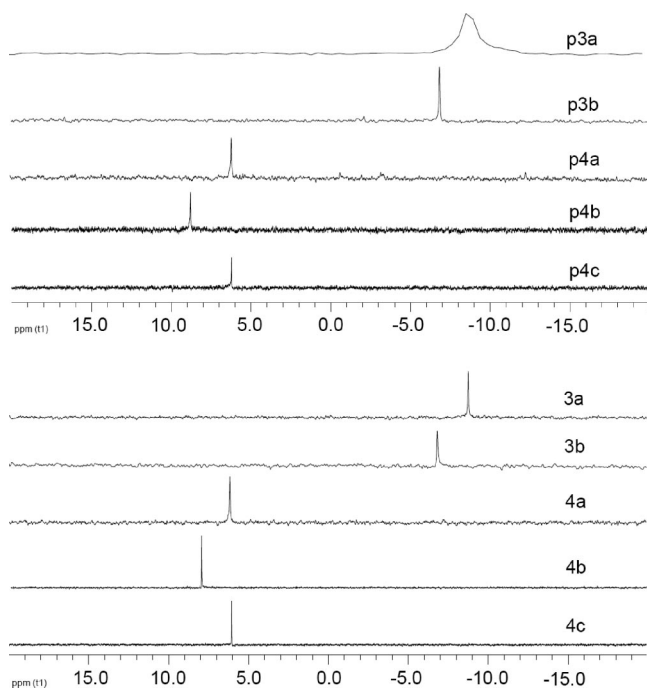


**Figure 3.**  $^{29}\text{Si}$  NMR (120 MHz in  $\text{CDCl}_3$ ; **p3a** in solid state) of silylenes (**3**), siloxanes (**4**), and their respective ADMET condensates (**p3** and **p4**).

**Table 4.**  $^{29}\text{Si}$  NMR Shifts of Silylene (**3**) and Siloxane (**4**) Monomers and Their Respective ADMET Condensates (**p3** and **p4**)

compound	-Si-		-Si-O-Si-		
	3a/p3a	3b/p3b	4a/p4a	4b/p4b	4c/p4c
$^{29}\text{Si}-\delta(\text{ppm})$	-8.75/-9.68 <sup>a</sup>	-6.84/-6.83	6.12/6.21	8.02/8.84	6.05/6.22

<sup>a</sup> Solid state.

pearance marked the degree of ADMET reaction. At the cost of the oop bending at  $\sim 987$  and  $\sim 906\text{ cm}^{-1}$  in the monomers

**Table 5.** Relative  $^{13}\text{C}$  NMR Integrals (Quantitative) of Silylene (**3b**) and Siloxane (**4a**) Monomers

C#	Assignment	3b exp. (theo.)	4a exp. (theo.)
1	1	1.55 (2)	4.13 (4)
2	2	1.14 (2)	3.83 (4)
3	3	1.08 (2)	4.40 (4)
4	4	1.53 (2)	4.7 (4)
5+6	5	2.81 (4)	9.86 (8)
7	6	1.13 (2)	5.08 (4)
8	7	1.42 (2)	4.88 (4)
9	8		
9	$-\text{CH}=\text{CH}_2$	2 <sup>+</sup> (2)	2 <sup>+</sup> (2)
10	$-\text{CH}=\text{CH}_2$	1.09 (2)	0.80 (2)
11		3.36 (4)	3.65 (4)
12		2.54 (4)	3.44 (4)
13		0.57 (2)	1.51 (2)
14		0.63 (2)	1.29 (2)

<sup>+</sup> Used as internal calibration.

a new signal appeared at  $\sim 965\text{ cm}^{-1}$ , indicating oop bending of the newly formed internal *trans*-vinylene bond. Broad vibration modes from Si-O at  $\sim 1075\text{ cm}^{-1}$  are observed in all **4** and **p4** cases and are clearly absent in samples of **3** and **p3**. Comprehensive FT-IR data are supplied in the Supporting Information.

On the basis of the strong evidence from the GPC (narrow molecular weight distributions and distinct molecular weight fractions),  $^1\text{H}$  NMR (absence of chain end functional vinyl

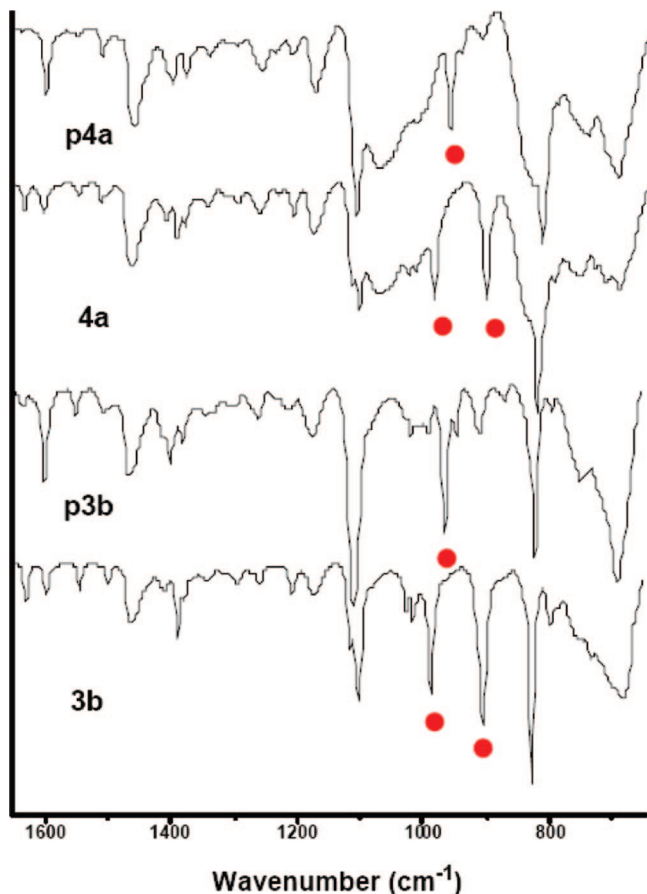


**Figure 4.** ATR-FTIR spectra (selected region) of silylene (**3b**) and siloxane (**4a**) monomers and their respective ADMET condensates (**p3** and **p4**).

groups), and  $^{13}\text{C}$  NMR (see also Supporting Information), it seems to be evident that the products **p3** represent the linear chain condensates of the ADMET process, whereas the products **p4** represent mainly the ring condensates of the ADMET backbiting process due to the highly flexible and long Si—O—Si linkages. Scheme 3 illustrates this.

The “dimeric” **p4b** ring has a theoretical  $M_n \sim 732$  g/mol compared to a measured  $M_n \sim 670$  g/mol vs polystyrene standards (average of two independent product batches in Table 1). The analogous “dimeric” **p4a** and **p4c** feature theoretical  $M_n$ 's of  $\sim 1405$  and  $\sim 893$  g/mol compared to measured averages of 1393 and 915 g/mol, respectively. The dimeric rings seem to present a product “trap” in the ADMET reaction. The GPC traces reveal additional but minor discrete fractions at higher molecular weights, corresponding to larger ring homologues (trimer, tetramer). The tailing in the traces toward higher molecular weights indicates small amounts of linear polycondensation products with broader molecular weight distributions.

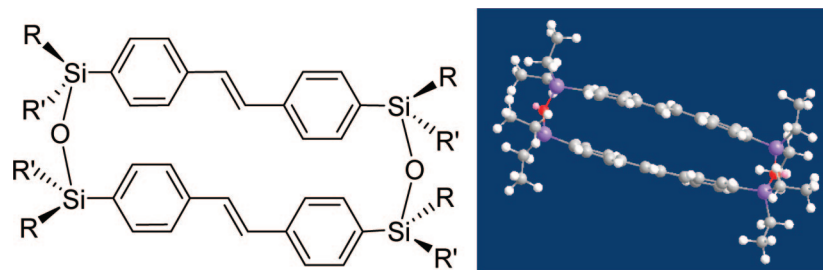
The presented systems highlight the ring—chain equilibrium nature of the ADMET reaction, dependent on the nature of the divinyl monomer.

**Optical Characterization.** The materials were investigated with regard to their optical properties. Figure 5 summarizes UV/vis absorption spectra together with photoluminescence (PL) spectra of monomers and ADMET condensates, together with *trans*-stilbene, recorded as hexane solutions.

All ADMET condensates showed absorptions with  $\lambda_{\text{max}} \sim 320\text{--}324$  nm, whereas the monomers absorbed with  $\lambda_{\text{max}} \sim 256\text{--}259$  nm. There is a  $\sim 60$  nm red shift from monomer to condensate, indicating an increase in the conjugated system. The aromatic unit formed is *trans*-stilbene in all condensates, regardless of monomer; isolated *trans*-stilbene absorbs with  $\lambda_{\text{max}} \sim 295$  nm,  $\sim 25\text{--}29$  nm blue-shifted relative to **p3** and **p4**. This is strong evidence for the participation of Si in the electronic conjugation of the aromatic units. Emission data are in line with the absorption behavior. The emission showed  $\lambda_{\text{max}} \sim 359\text{--}360$  nm for all ADMET condensates compared to  $\lambda_{\text{max}} \sim 306\text{--}307$  nm in the case of the monomers; thus, there is a  $\sim 52\text{--}59$  nm red shift from monomers to condensates. The pure *trans*-stilbene shows emission with  $\lambda_{\text{max}} \sim 347$  nm, thus  $\sim 13\text{--}19$  nm blue-shifted relative to **p3** and **p4** and in accordance with the absorption findings. Absorption and emission of **p3** and **p4** do not overlap too much (not shown), resulting in effective fluorescence properties. The fluorescence quantum yields of the polymers (on a repeat unit basis) are 5-fold higher than the reported value for the model compound *trans*-stilbene. This may be due to the influence of Si on the conjugation, although there seems to be no significant difference between the silylene systems **p3** and the siloxanes **p4**. The observed absorption coefficients in the **p4** systems were always significantly higher than the **p3** systems, whereas the quantum efficiencies showed no significant differences. In the case of **p3a** more low-energy components were observed in the emission, as is expected from the low bulk of the substituents on the Si link.<sup>13,18</sup> In most cases, concentration-dependent emission spectra did not yield much change in the emission; i.e., only minor low-energy components were observed at higher concentrations. This leads to the conclusion that in the case of **p3b** the steric bulk from the octyl chains on the Si moiety is bulky enough to prevent interchain aggregation. In the cases of **p4**, the aromatic segments in the ring are shielded efficiently from other rings by the side chains on the Si that radiate away from the ring. The optical properties are summarized in Table 6.

**Thermal.** The thermal stability of the ADMET condensates under nitrogen was investigated by means of thermogravimetric analysis (TGA) as shown in Figure 6. The stabilities showed no distinct trend based on the side chain substitution R and R' at the Si and varied from temperatures for the 95% weight loss of  $\sim 125$  °C in the case of **p4c** to 333 °C in the case of **p3a**. On average, however, the silylene-based systems seem to be more stable than the siloxane systems.

**Scheme 3.** Cyclic Dimer **p4**: General Structure (left) and Model of **p4b** (right)





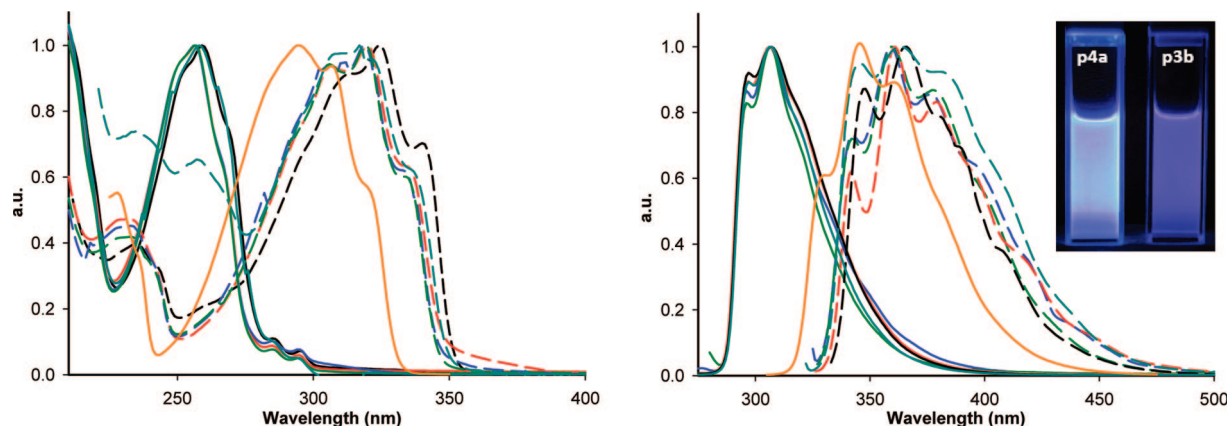


**Figure 5.** UV/vis absorption spectra (left) and emission spectra (right) of silylene monomers [**3a** (cyan), **3b** (black)] and siloxane monomers [**4a** (red), **4b** (blue), **4c** (green)], their respective ADMET condensates [**p3a**, **p3b**, **p4a**, **p4b**, **p4c** (dashed lines)], and *trans*-stilbene (orange); excitation at the respective absorption maxima; solutions in hexane.

**Table 6.** UV/Vis and Emission of Monomers **3** and **4** and ADMET Products **p3** and **p4** (Solutions in Hexane)

monomers			ADMET condensates				
	$\lambda_{\text{max,UV/vis}}$ (nm)	$\lambda_{\text{max,emission}}$ (nm)		$\epsilon$ (L mol <sup>-1</sup> cm <sup>-1</sup> )	$\lambda_{\text{max,UV/vis}}$ (nm)	$\lambda_{\text{max,emission}}$ (nm)	$\Phi_{\text{eff}}$ (%) <sup>c</sup>
<b>3a</b>	258	307	<b>p3a</b>	n.a.	317	363	n.a.
<b>3b</b>	259	307	<b>p3b</b>	22 881	324	366	24
<b>4a</b>	257	306	<b>p4a</b>	37 580	320	360	28
<b>4b</b>	256	306	<b>p4b</b>	24 851	319	359	25
<b>4c</b>	257	307	<b>p4c</b>	35 104	319	359	24
			<i>trans</i> -stilbene	29 000 <sup>a</sup>	295	347	5 <sup>b</sup>

<sup>a</sup> Reference 18. <sup>b</sup> Reference 20. <sup>c</sup> Relative to Rhodamine B solutions in H<sub>2</sub>O.<sup>21</sup>

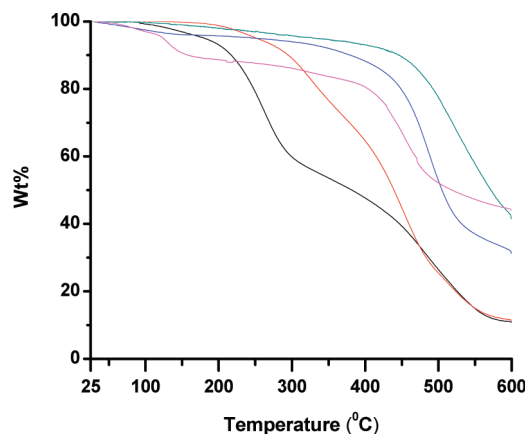


**Figure 6.** TGA traces (10 °C/min in N<sub>2</sub>) of **p3a** (green), **p3b** (purple), **p4a** (orange), **p4b** (black), and **p4c** (red).

## Conclusion

Silylene- and siloxane-functional conjugated polymers and macrocycles could be accessed via ADMET condensation. The organic conjugated segment formed was stilbene with only *trans*-configured vinylene bonds. The flexible siloxane linkage in monomers **4** resulted exclusively in macrocycles under presented reaction conditions, while the silylene linkage in monomers **3** led to linear polycondensates. Photophysical characterization of the products showed the participation of Si in the conjugation, in both the siloxanes and silylenes. Further investigations currently under way include using different heteroatom linkages and varying reaction conditions to influence the ring/chain equilibria of the ADMET reaction.

## Experimental Section

**Materials.** Magnesium turnings, *n*-BuLi [2.5 M in hexane], 4-bromobenzaldehyde dimethylacetal (98%), triphenylphosphonium methyl bromide, sodium sulfate, sodium bicarbonate, sodium

chloride, acetic acid, and Grubbs–Hoveyda catalyst were obtained from Aldrich. *p*-Bromostyrene (98%) was obtained from Alfa Aesar, and dichlorodioctylsilylene was obtained from Gelest Inc. Magnesium turnings were flame-dried under high vacuum prior to use. Solvents such as tetrahydrofuran (THF), toluene, hexane, and diethyl ether were purchased from Fisher Scientific. Except for diethyl ether, all other solvents were dried and degassed by a “Pure Solv” solvent purification system (using activated alumina, copper catalyst, molecular sieves column.) by Innovative Technology Inc. before use. All other chemicals were used as received. Column chromatography was carried out on silica gel 60 (70–230 mesh) from EMD Chemicals Inc.

**Synthetic Procedures (Multiple).** *Synthesis of Dibenzaldehyde Dioctylsilylene.* 40 mmol of 4-bromobenzaldehyde dimethylacetal was dissolved in 50 mL of dry THF. The temperature was lowered to −78 °C. 40 mmol of <sup>n</sup>BuLi [2.5 M in hexane, 16 mL] was slowly added. The reaction was stirred for 1.5 h at −78 °C. 19.5 mmol of dichlorodioctylsilylene in 5 mL of THF was then added, the reaction was continued for 12 h, and the mixture was finally warmed up gradually to room temperature. The reaction mixture was concentrated, washed with brine, and extracted twice with diethyl ether. The organic fractions were combined, dried over sodium sulfate, and concentrated to a crude oil of the diacetal of dibenzaldehyde dioctylsilylene.

This crude oil was then mixed with 20 mL of acetic acid and 25 mL of water and stirred for 5 h at 40 °C. The resulting reaction mixture was neutralized with saturated sodium bicarbonate solution and then extracted with diethyl ether. The organic fractions were further washed with brine, dried over sodium sulfate, and concentrated to afford the dibenzaldehyde dioctylsilylene as light yellow oil. Yield 85% [based on dichlorosilylene used]. <sup>1</sup>H NMR (CDCl<sub>3</sub>, ppm): 0.84 (t, *J* = 7 Hz, 6H), 1.0–1.3 (m, 28H), 7.62 (d, *J* = 6.9 Hz, 4H), 7.82 (d, *J* = 6.9 Hz, 4H), 10.01 (s, 2H). <sup>13</sup>C NMR (CDCl<sub>3</sub>, ppm): 192.49, 144.50, 136.8, 135.27, 128.7, 33.52, 31.82, 29.13, 29.05, 23.49, 22.61, 14.1, 11.96. <sup>29</sup>Si NMR (CDCl<sub>3</sub>, ppm): −5.47.

*Synthesis of Dibenzaldehyde Dimethylsilylene.* The same procedure was followed as mentioned above for dibenzaldehyde dioctylsilylene. The crude product was purified by recrystallization from a hexane/ethyl acetate (4:1) mixture to obtain a crystalline

material consisting of white needles. Yield 88% [based on dichlorosilylene used].  $^1\text{H}$  NMR ( $\text{CDCl}_3$ , ppm): 0.62 (s, 6H), 7.65 (d,  $J = 7.88$  Hz, 4H), 7.83 (d,  $J = 7.87$  Hz, 4H), 10.01 (s, 2H).  $^{13}\text{C}$  NMR ( $\text{CDCl}_3$ , ppm): 192.42, 145.61, 136.89, 134.66, 128.8, -2.84.  $^{29}\text{Si}$  NMR ( $\text{CDCl}_3$ , ppm): -6.6.

**Synthesis of Diocetylidyldistyrilsilylene (3b).** To a suspension of 35 mmol of triphenylphosphonium methyl bromide in 100 mL of dry THF, 30 mmol of *n*-BuLi [2.5 M in hexane, 12 mL] was slowly added at 0 °C. The reaction mixture was stirred for 3 h. To this resulting solution, 10 mmol of dibenzaldehyde diocetylidyldistyrilsilylene dissolved in 10 mL of dry THF was slowly added at 0 °C. The resulting mixture was stirred for 12 h and then washed with brine. The organic phase was extracted with diethyl ether twice, dried over sodium sulfate, and concentrated to yield a crude oil of the diocetylidyldistyrilsilylene, which was purified by passing through a silica gel column using hexane as an eluent to obtain a colorless liquid. Yield 66%.  $^1\text{H}$  NMR ( $\text{CDCl}_3$ , ppm): 0.9 (t,  $J = 7$  Hz, 6H), 1.0–1.2 (m, 4H), 1.2–1.5 (m, 24H) 5.26 (d,  $J = 11.2$  Hz, 2H), 5.79 (d,  $J = 17.7$  Hz, 2H), 6.72 (dd,  $J = 11.2$  Hz, 17.7 Hz, 2H), 7.39 (d,  $J = 8.1$  Hz, 4H), 7.47 (d,  $J = 7.8$  Hz, 4H).  $^{13}\text{C}$  NMR ( $\text{CDCl}_3$ , ppm): 138.1, 136.9, 136.4, 135.1, 125.51, 114.2, 33.73, 31.9, 29.25, 29.15, 23.69, 22.66, 14.1, 12.55.  $^{29}\text{Si}$  NMR ( $\text{CDCl}_3$ , ppm): -6.84.

**Synthesis of Dimethyldistyrilsilylene (3a).** The same procedure was followed as mentioned above for diocetylidyldistyrilsilylene (3b) to obtain a colorless liquid. Yield 66%.  $^1\text{H}$  NMR ( $\text{CDCl}_3$ , ppm): 0.6 (s, 6H), 5.30 (d,  $J = 10.8$  Hz, 2H), 5.82 (d,  $J = 18.6$  Hz, 2H), 6.75 (dd,  $J = 10.8$  Hz, 18.6 Hz, 2H), 7.44 (d,  $J = 7.8$  Hz, 4H), 7.54 (d,  $J = 8.1$  Hz, 4H).  $^{13}\text{C}$  NMR ( $\text{CDCl}_3$ , ppm): 138.21, 137.73, 136.74, 134.38, 125.57, 114.29, -2.42.  $^{29}\text{Si}$  NMR ( $\text{CDCl}_3$ , ppm): -8.75.

**Synthesis of Diocetylidyldistyrilsiloxane (4a).** To a solution of (5.86 g, 32 mmol) of *p*-bromostyrene in 70 mL of dry THF, flame-dried magnesium turnings (1.54 g, 64 mmol) and a few iodine crystals were added. The solution was refluxed under constant stirring. After 6 h the reaction mixture was cooled to room temperature and transferred to another vessel using a pipet. A solution containing 4.30 g (16 mmol) of dichlorodistyrilsilylene in 20 mL of dry THF was slowly added. The reaction mixture was stirred for 16 h at room temperature. After the reaction was complete, 0.1 M HCl solution was added dropwise until the formation of precipitate ceased. The suspension was quickly filtered, and the filtrate was hydrolyzed with 200 mL of distilled water followed by extraction with 100 mL of diethyl ether. The organic layer was collected, washed twice with 100 mL of distilled water, and then dried over magnesium sulfate. Finally, the solvent was removed under vacuum, and the resulting crude product was purified by column chromatography (silica gel with hexane/methyl *tert*-butyl ether [95:5] as an eluent) to obtain 3 as a pale yellow liquid. The yield was 2.6 g (36%).  $^1\text{H}$  NMR ( $\text{CDCl}_3$ , ppm): 0.52–1.3 (m, 34H), 5.25 (d,  $J = 11$  Hz, 2H), 5.75 (d,  $J = 17.4$  Hz, 2H), 6.7 (dd,  $J = 11$  Hz, 17.4 Hz, 2H), 7.34–7.53 (m, 8H).  $^{13}\text{C}$  NMR ( $\text{CDCl}_3$ , ppm): 138.49, 137.43, 136.8, 133.7, 125.6, 114.35, 33.48, 31.87, 29.21, 22.95, 22.65, 15.78, 15.18, 14.1.  $^{29}\text{Si}$  NMR ( $\text{CDCl}_3$ , ppm): 6.12.

**Synthesis of Diethyldistyrilsiloxane (4b).** The same procedure was followed as mentioned above for diocetylidyldistyrilsiloxane (4a) to obtain a colorless liquid. Yield 51%.  $^1\text{H}$  NMR ( $\text{CDCl}_3$ , ppm): 0.86 (m, 8H), 1.01 (t,  $J = 7.8$  Hz, 12H) 5.29 (d,  $J = 12$  Hz, 2H), 5.81 (d,  $J = 24$  Hz, 2H), 6.74 (dd,  $J = 12$  Hz, 24 Hz, 2H), 7.42 (d,  $J = 7.8$  Hz, 4H), 7.55 (d,  $J = 8.4$  Hz, 4H).  $^{13}\text{C}$  NMR ( $\text{CDCl}_3$ , ppm): 138.4, 137.1, 136.1, 135.41, 125.8, 114.5, 7.7, 4.16.  $^{29}\text{Si}$  NMR ( $\text{CDCl}_3$ , ppm): 8.04.

**Synthesis of Methylcyclohexyldistyrilsiloxane (4c).** The same procedure was followed as mentioned above for diocetylidyldistyrilsiloxane (4a) to obtain a colorless liquid. Yield 41%.  $^1\text{H}$  NMR ( $\text{CDCl}_3$ , ppm): 0.34 (s, 6H), 0.87–0.91 (m, 2H), 1.1–1.25 (m, 10H) 1.65–1.75 (m, 12H) 5.26 (d,  $J = 11.6$  Hz, 2H), 5.78 (d,  $J = 17.6$  Hz, 2H), 6.71 (dd,  $J = 11.6$  Hz, 17.6 Hz, 2H), 7.4 (d,  $J = 8$  Hz, 4H), 7.51 (d,  $J = 8.04$  Hz, 4H).  $^{13}\text{C}$  NMR ( $\text{CDCl}_3$ , ppm): 138.25,

137.14, 133.97, 129.1, 125.86, 27.75, 26.76, 26.67, -3.62.  $^{29}\text{Si}$  NMR ( $\text{CDCl}_3$ , ppm): 6.05.

**Typical Synthesis of p3b.** 360 mg (0.78 mmol) of diocetylidyldistyrilsilylene and 2.5 mol % of Grubbs second generation catalyst were placed in an air-free reaction tube and dissolved in 2 mL of dry toluene. The reaction mixture was heated at 48 °C for 18 h. Ethylene gas (byproduct) was removed by applying vacuum intermittently. A viscous reaction mixture formed, which was cooled down to room temperature. To this resulting viscous mixture 5 mL of ethyl ether was added. The diluted solution was passed through a short silica gel column to remove the catalyst residue (using ethyl ether as an eluent). Finally, all volatiles were removed to yield 320 mg of greenish-black polymer as a semisolid (p3b).  $^1\text{H}$  NMR ( $\text{CDCl}_3$ , ppm): 0.57–1.38 (m), 5.26 (d, 5.78 (d), 6.6–6.9 (m), 7.13 (s), 7.47–7.57 (m).  $^{13}\text{C}$  NMR ( $\text{CDCl}_3$ , ppm): 138.2, 137.4, 133.84, 129.08, 125.91, 33.47, 31.88, 29.20, 22.96, 22.64, 15.79, 15.19, 14.09.  $^{29}\text{Si}$  NMR ( $\text{CDCl}_3$ , ppm): -6.83.

**Synthesis of p3a.** The same procedure was followed as mentioned above for p3b. During the polymerization an off-white solid formed. The reaction mixture was poured over a large amount of ice-cold methanol and stirred for an hour. The product was filtered and dried in vacuum for 24 h to obtain an off-white powder.  $^1\text{H}$  NMR ( $\text{CDCl}_3$ , ppm): 0.53 (s), 0.54 (s), 5.24 (d,  $J = 10.85$  Hz), 5.76 (d,  $J = 17.6$  Hz), 6.7 (dd,  $J = 10.85$  Hz, 17.6 Hz), 7.1 (s), 7.48 (m).  $^{13}\text{C}$  NMR (solid state, ppm): 136.47, 134.43, 124.8, 114.32, -3.93.  $^{29}\text{Si}$  NMR (solid state, ppm): -9.68.

**Synthesis of p4a.** The same procedure was followed as mentioned above for p3b to obtain a greenish-black semisolid material as product.  $^1\text{H}$  NMR ( $\text{CDCl}_3$ , ppm): 0.52–1.4 (m), 7.13 (s), 7.45–7.58 (m, 8H).  $^{13}\text{C}$  NMR ( $\text{CDCl}_3$ , ppm): 138.2, 137.4, 133.8, 129.1, 125.9, 33.48, 31.88, 29.21, 22.95, 22.65, 15.78, 15.2, 14.1.  $^{29}\text{Si}$  NMR ( $\text{CDCl}_3$ , ppm): 6.12.

**Synthesis of p4b.** The same procedure was followed as mentioned above for p3b to obtain a greenish-black solid material as product.  $^1\text{H}$  NMR ( $\text{CDCl}_3$ , ppm): 0.86 (t) 0.95–1.1 (m) 7.41–7.58 (d).  $^{13}\text{C}$  NMR ( $\text{CDCl}_3$ , ppm): 138.28, 136.75, 133.93, 129.1, 125.94, 6.57, 6.4.  $^{29}\text{Si}$  NMR ( $\text{CDCl}_3$ , ppm): 8.04.

**Synthesis of p4c.** The same procedure was followed as mentioned above for p3b to obtain a greenish-black semicrystalline material as product.  $^1\text{H}$  NMR ( $\text{CDCl}_3$ , ppm): 0.35 (s), 0.88–0.95 (br), 0.98–1.3 (m), 1.4–1.8 (m), 7.39 (d,  $J = 8$  Hz, 4H), 7.13 (s), 7.41–7.57 (m).  $^{13}\text{C}$  NMR ( $\text{CDCl}_3$ , ppm): 138.3, 137.1, 134, 129.1, 125.9, 27.8, 26.8, 26.7, -3.6.  $^{29}\text{Si}$  NMR ( $\text{CDCl}_3$ , ppm): 6.05.

**Measurements.** 200, 300, or 600 MHz  $^1\text{H}$  NMR, 50, 75, or 150 MHz  $^{13}\text{C}$  NMR, and 120 MHz  $^{29}\text{Si}$  NMR spectra were recorded in  $\text{CDCl}_3$  on Varian Unity NMR instruments.  $\text{CDCl}_3$  was used as an internal deuterium lock for  $^1\text{H}$  NMR,  $^{13}\text{C}$  NMR, and  $^{29}\text{Si}$  NMR spectra. All of the signals in the NMR spectra are reported in ppm. Quantitative  $^{13}\text{C}$  NMR was carried out in presence of a 50 mM relaxation agent [tris(acetylacetonato)chromium(III)] with a pulse delay time of 20 s. UV/vis absorption spectra were recorded using a Perkin-Elmer Model 650 UV spectrophotometer with 1 cm path length cells. The samples were prepared with HPLC grade chloroform ("Spectrasolv") in a sample cell. Infrared spectra were recorded on a Tensor 27 Fourier transformed infrared spectrometer from Bruker Optics using a Pike ATR accessory; data were processed and analyzed by OPUS software. Photoluminescence spectra were recorded using a Horiba Jobin Yvon Fluoromax-3 spectrofluorometer with 1 cm path length cells. The samples were prepared with HPLC grade chloroform ("Spectrasolv") in a sample cell. Thermogravimetric analysis was carried out on a Hi-Res TGA 2950 thermogravimetric analyzer from TA Instruments using a platinum pan with a heating rate 10 °C/min under continuous flow of nitrogen. GPC analysis was carried out on an Alliance GPCV 2000 (Waters) instrument equipped with four Waters Styragel HR columns, i.e., HR-1, HR-3, HR-4, and HR-5E. HPLC grade THF was used as eluent at a flow rate of 1.0 mL/min at 40 °C. Measurements are relative to polystyrene standards.

**Acknowledgment.** The authors thank Dr. Hsin Wang for help and numerous discussions with the NMR experiments. Funding was



provided by CUNY/CSI startup funds, a CUNY Collaborative Incentive grant, and a PSC/CUNY research award.

**Supporting Information Available:** Additional  $^1\text{H}$  NMR,  $^{13}\text{C}$  NMR, FTIR spectra with assignments. This material is available free of charge via the Internet at <http://pubs.acs.org>.

## References and Notes

- (1) Nespurek, S. *J. Non-Cryst. Solids* **2002**, 299–302, 1033.
- (2) (a) Tanaka, K.; Ago, H.; Yamabe, T.; Ishikawa, M. T.; Ueda, T. *Organometallics* **1994**, 5583. (b) Pohl, A.; Bredas, J.-L. *Int. J. Quantum Chem.* **1997**, 63, 437.
- (3) (a) Jung, S. H.; Kim, H. K.; Kim, S. H.; Kim, Y. H.; Jeoung, S. C.; Kim, D. *Macromolecules* **2000**, 33, 9277. (b) Paik, K. L.; Baek, N. S.; Kim, H. K.; Lee, Y.; Lee, K. J. *Thin Solid Films* **2002**, 417, 132. (c) Kim, H. K.; Park, J.-S.; Kim, K.-D.; Jung, S.-H.; Jeoung, S. C.; Kim, Y. H.; Kim, D. *Mol. Cryst. Liq. Cryst. Sci. Technol., Sect. A* **1999**, 327, 175.
- (4) (a) Ryu, M. K.; Kim, K. D.; Lee, S. D.; Cho, S. W.; Park, J. W. *Macromolecules* **1998**, 31, 1114. (b) Bruma, M.; Hamciuc, E.; Schulz, B.; Kopnick, T.; Kaminorz, Y.; Robison, J. J. *Appl. Polym. Sci.* **2003**, 87, 714. (c) Takagi, K.; Kunii, S.; Yuki, Y. *J. Polym. Sci., Part A: Polym. Chem.* **2005**, 43, 2119. (d) Kanemitsu, Y. In *Photonic Polymer Systems (Plastics Engineering)*; Wise, D. L., Wnek, G. E., Trantolo, D. J., Cooper, T. M., Gresser, J. D., Eds.; Marcel Dekker: New York, 1998; Vol. 49, pp 1–32.
- (5) Kwak, G.; Masuda, T. *Macromol. Rapid Commun.* **2002**, 23, 68.
- (6) (a) Sakurai, H.; Sugiyama, H.; Kira, M. *J. Phys. Chem.* **1990**, 94, 1837. (b) Chen, R.-M.; Chien, K.-M.; Wong, K.-T.; Jin, B.-Y.; Luh, T.-Y.; Hsu, J.-H.; Fann, W. *J. Am. Chem. Soc.* **1997**, 119, 11321. (c) Chen, Z.-K.; Lai, Y.-H.; Chan, H. S.-O.; Ng, S.-C.; Huang, W. *Chem. Lett.* **1999**, 6, 477. (d) Sumiya, K.-I.; Kwak, G.; Sanda, F.; Masuda, T. *J. Polym. Sci., Part A: Polym. Chem.* **2004**, 42, 2774.
- (7) Li, H.; Powell, D. R.; Firman, T. K.; West, R. *Macromolecules* **1998**, 31, 1093.
- (8) (a) Garnier, F. *Chem. Phys.* **1998**, 227, 253. (b) Mercuri, F.; Re, N.; Sgamellotti, A. *THEOCHEM* **1999**, 489, 35. (c) Garten, F.; Hilberer, A.; Cacialli, F.; Esselink, F. J.; Van Dam, Y.; Schlatmann, A. R.; Friend, R. H.; Klapwijk, T. M.; Hadzioannou, G. *Synth. Met.* **1997**, 85, 1253. (d) Yamashita, H.; de Leon, M. S.; Channasanon, S.; Suzuki, Y.; Uchimar, Y.; Takeuchi, K. *Polymer* **2003**, 44, 7089. (e) Mori, A.; Takahisa, E.; Kajiro, H.; Nishihara, Y.; Hiyama, T. *Macromolecules* **2000**, 33, 1115.
- (9) Representative review: (a) Yamaguchi, S.; Tamao, K. Sigma- and pi-conjugated organosilicon polymers. In *Silicon-Containing Polymers*; Jones, R. G., Ando, W., Chojnowski, J., Eds.; Kluwer Academic: Dordrecht, 2000; pp 461–498. (b) Kunai, A. *Organomet. News* **2007**, 3, 82, and references therein.
- (10) Kwak, G.; Takagi, A.; Fujiki, M. *Macromol. Rapid Commun.* **2006**, 27, 1561.
- (11) (a) Smith, D. W.; Wagener, K. B. *Macromolecules* **1993**, 26, 1633. (b) The new “bible”: *Handbook of Olefin Metathesis*; Grubbs, R. H., Ed.; Wiley-VCH: Weinheim, 2003; Vols. 1–3.
- (12) Marciniak, B. *Coord. Chem. Rev.* **2005**, 249, 2374.
- (13) Miao, Y. J.; Bazan, G. C. *Macromolecules* **1997**, 30, 7414.
- (14) Mukherjee, N.; Peetz, R. M. *Polym. Prepr. (Am. Chem. Soc., Div. Polym. Mater. Sci. Eng.)* **2006**, 94, 822.
- (15) Kumagai, T.; Itsuno, S. *Tetrahedron: Asymmetry* **2001**, 12, 2509.
- (16) Kvaranl, A.; Konradsson, A. E.; Evans, C.; Gerisson, J. K. F. *J. Mol. Struct.* **2000**, 553, 79.
- (17) Marsmann, H.  $^{29}\text{Si}$ -NMR spectroscopic results. In *NMR. Basic Principles and Progress*; Diehl, P., Fluck, E., Kosfeld, R., Eds.; Springer-Verlag: Berlin, 1981; Vol. 17, pp 65–235.
- (18) Kalyanasundaram, K. *Photochemistry in Microheterogeneous Systems*; Academic Press: New York, 1987.
- (19) Beale, R. N.; Roe, E. M. F. *J. Chem. Soc.* **1953**, 2755.
- (20) Allen, M. T.; Whitten, D. G. *Chem. Rev.* **1989**, 89, 1691.
- (21) Lakowicz, J. R. *Principles of Fluorescence Spectroscopy*, 3rd ed.; Springer: Berlin, 2006.

MA800671G